

Section 7: Electrothermal Propulsion

AE435
Spring 2018

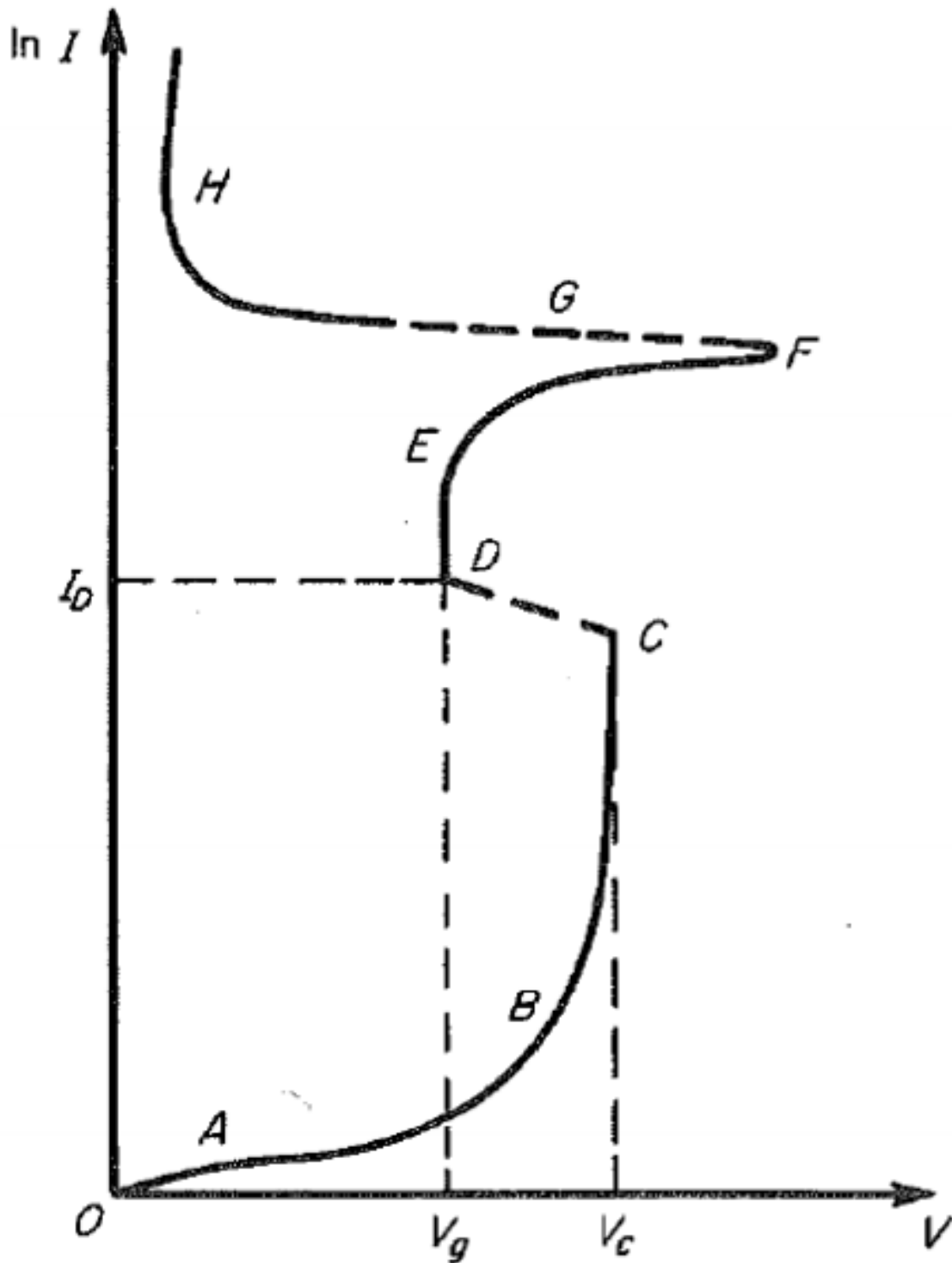
2 Arcjets

Contents

2	Arcjets	37
2.1	Discharge Physics	38
2.2	Arc Physics	45
2.3	Modeling Approaches	52
2.3.1	Core Flow Model	52
2.3.2	Heat Transfer:	54

2.1 Discharge Physics

Figure 6-12 in Jahn shows the electrical characteristic for a gaseous discharge. Starting at the lowest discharge current and heading upwards:



1. **O-A: The Stray Charge Region**, here, ionization of gas is by background radiation, electrodes simply pick up bits of stray charge. There is very little ionization in this region. All the charged particles that we are collecting are due to stray ionization.
2. **A-B: The First Townsend Region**, where stray electrons pick up enough kinetic energy between collisions to ionize gas. The current, $J \propto$ External Radiation Source Intensity, and so this is where Geiger-Muller counters operate. The electron has ionization collision with background neutral. We have enough electric field in this gap that any electron that gets created, now they are getting accelerated by that gap and have enough energy to collide.
3. **B-C: The Second Townsend Region**, where ions pick up enough kinetic energy from the E-field to cause **secondary electron emission** from the cathode. In this gap, ions pick up enough kinetic energy, a secondary electron comes off that cathode. The electron now accelerated towards the anode in the opposite direction. As it goes along that path it will have ionization collisions and create more ions.

Figure 12:

4. **C-D: Sparking and Discharge Region**, electron avalanche, lots of ionization and secondary electron emission. A self sustaining process of "steady discharge". The sparking discharge region curve here depends on
 - Power supply characteristics
 - Gas pressure
 - Electrode material - Determines the secondary electron emission
 - Electrode shape
 - Sharp points and/or high pressure lead to a **corona discharge**.

Figure 13:

- Blunt electrodes and/or low pressure lead to a **glow discharge**.

Figure 14:

- Electrode spacing

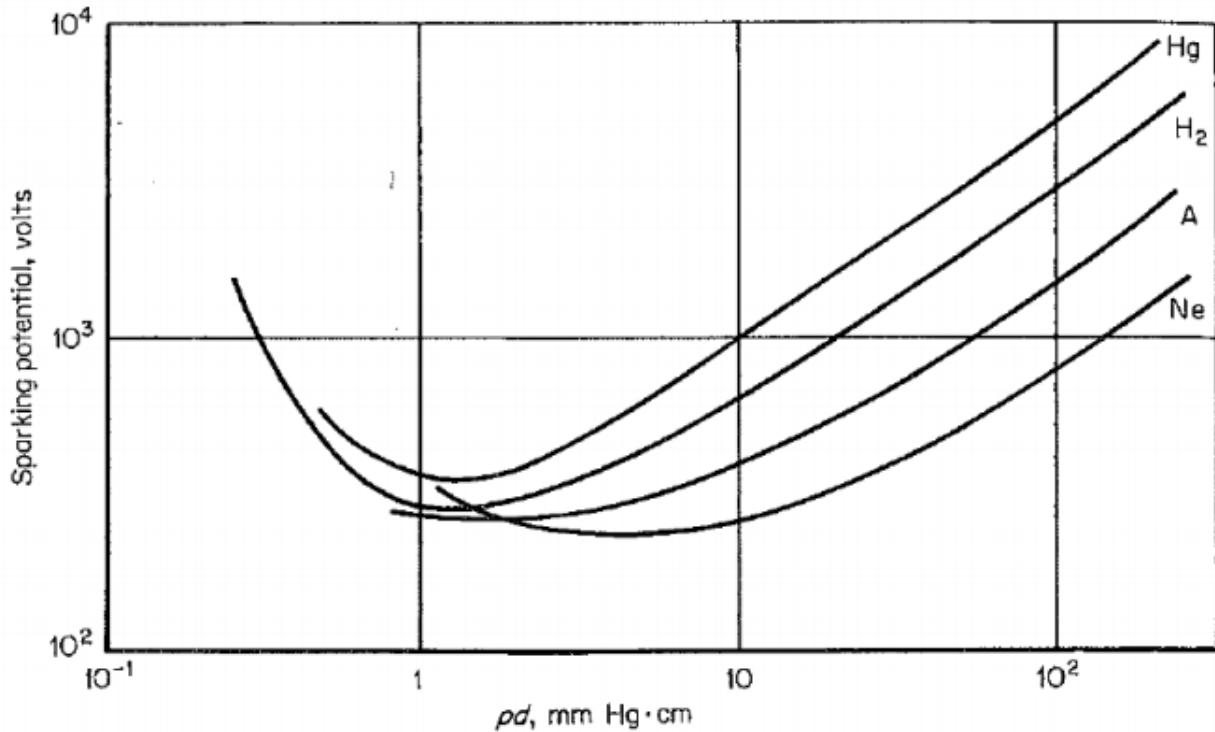


Fig. 6-13 Sparking potential for various gases (Paschen's law). (From A. von Engel, "Ionized Gases," chap. 7, p. 172, Oxford University Press, Fair Lawn, N.J., 1955.)

From this figure, we have the relation between the gas pressure, electrode spacing and sparking potential. The voltage potential that is needed to get from region C to D. Figure 6-13 in Jahn shows "Paschen curve" of V_c as a function of $p d$, where

- p is the pressure
- d is the electrode gap

5. **D-E: Normal Glow Discharge Region**, characterized by:

- Constant current density (10^{-3} to 1 A/cm^2)
- High T_e and low $T_i \sim T_A$
- Voltage drop primarily in cathode sheath

6. **E-F: Abnormal Glow Discharge Region**, where the

- Cathode drop starts to increase with current
- Cathode heating grows proportionally

7. **F-G: Glow-to-Arc Transition Region**, where the cathode temperature T_c increase until thermionic emission starts to predominate. Now, the cathode is really giving off electrons. Not only do we have secondary electron emissions but now since the cathode is so hot, electrons are popping off the surface because it so hot. "Thermionic Emission", meaning temperature driven emission. Also, field emission helps this process as well. If we have the cathode, there is also a plasma sheath that forms around the cathode. There will be a large potential drop that is relatively thin where the voltage drops orders of magnitude. As a result we have really strong electric fields right there at the surface. So we have a really strong field and the high temperature wanting to push electrons off the surface. The governing equation for this is:

Richardson-Dushman Relation

$$j_e = A_r T_c^2 \exp \left[\frac{-\Phi_{eff}}{k T_c} \right] \quad (7.72)$$

Where

$$A_r = 60 \left[\frac{A}{cm^2 K^2} \right] \quad (7.73)$$

and...

Effective Work Function

$$\Phi_{eff} = \Phi_w - \sqrt{\frac{q_e E_c}{4 \pi \epsilon_o}} \quad (7.74)$$

Where

Φ_w = Zero-Field Work Function

E_c = Electric-Field Magnitude at the Cathode Surface

Equation 7.74, the field reduces the work function required to push electrons off the surface. Φ_{eff} decreases the larger that electric field is. It is easier to pop the electrons off the surface.

Lowering the work function increase the emission current density.

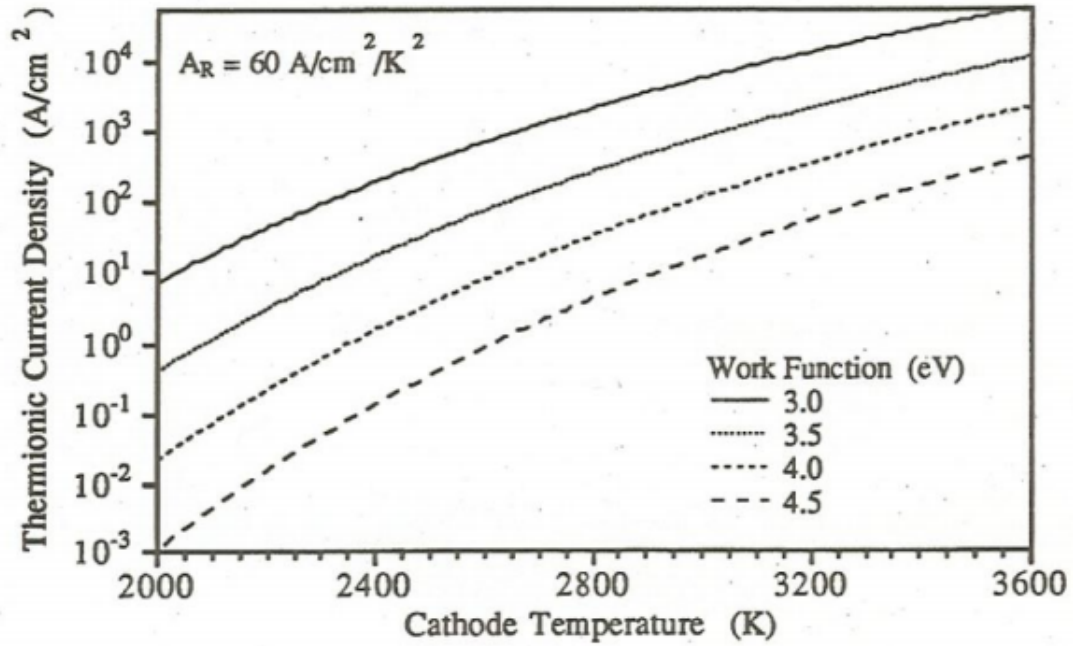


Figure 2.2: Effect of material work function on thermionic emission current.

Typical work functions for metal surfaces:

Metal	Φ_w (V)
Si	4.90
Ni	4.50
Mo	4.30
W	4.54

Mo and W are typically used in EP systems and often used for cathode materials.

Increased electric field has the same effect as lower work function:

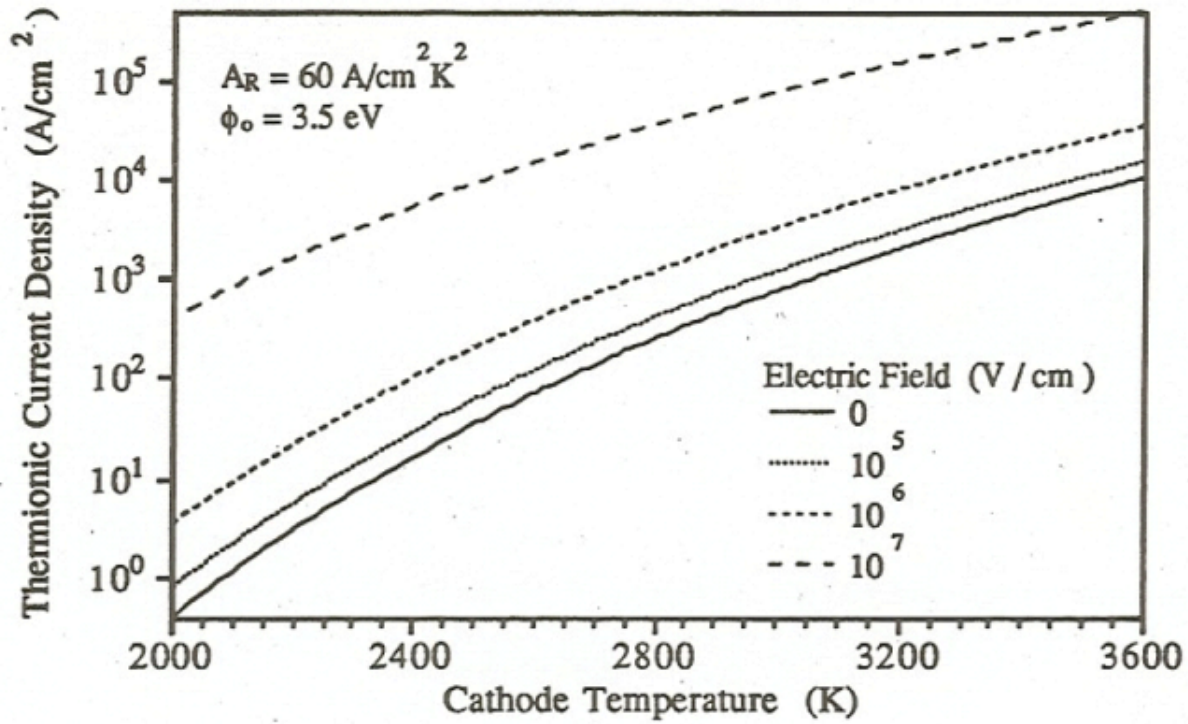
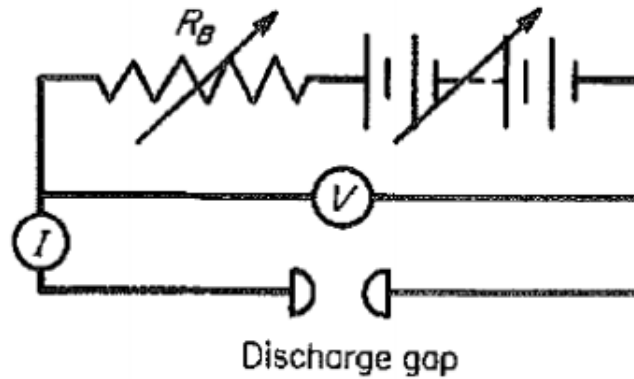


Figure 2.3: Effect of surface electric field on thermionic emission current.

Once thermionic emission sets in, the cathode drop decreases and the current increases. The cathode temperature (and, thus, the emission current density) is regulated by the energy balance:

- Heating: Ion bombardment and radiation
- Cooling: Conduction (to gas and solids), radiation, convection and electron emission

8. **G-H: Arc**, with resistance dropping rapidly enough that prompt kA currents, can vaporize electrodes. Classic fix, place a ballast resistor in series with the circuit:



$$V_B = I R_B$$

$$V_{tot} = V_B + V_{gap}$$

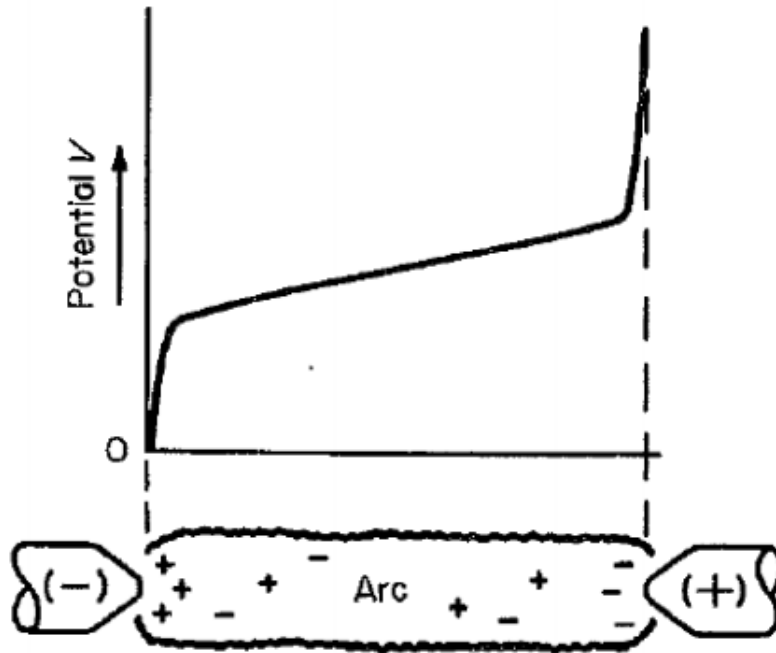
As the current increases, the voltage drop across R_B increases, preventing "runaway".

Note that G-H is the regime of interest for Electrothermal Thrusters Arcjet propulsion.

In this figure, we have the set up for an arc jet. We have a voltage applied across some discharge gap, between the two electrodes. We have some low pressure region between that discharge gap.

2.2 Arc Physics

As we noted previously, an arc is struck when thermionic emission causes runaway current. Figure 6-15 in Jahn shows a schematic structures of an arc potential profile:



Features:

1. **Cathode Sheath**, usually
 - (a) A few Debye lengths λ_D thick
 - (b) A cathode fall, $V_c \sim \varepsilon_i$, cathode fall on the order of the ionization potential, this is the only region with significant ion current; ions pick up enough energy in the cathode fall to keep the cathode hot and emitting.
2. **Arc Column**, usually
 - (a) Quasineutral, with ionization fraction 10-100
 - (b) Near Complete Thermodynamic equilibrium, CTE, $T_e \sim T_n$
 - (c) Electron current dominates here (no ion current)
3. **Anode Sheath**, usually
 - (a) A few Debye lengths λ_D thick
 - (b) Anode Fall, V_a
 - i. Electron-accelerating sheath,
 - ii. Electron-repelling sheath, where column is more positive than anode.

Figure 15:

Question: Why would arc column have higher potential than the anode, (Common in a lot of DC plasmas)?

Answer: Electrons are a mobile species, they will leave the plasma and leave behind a little bit of extra ion charge. This will cause the ions in the sheath to form like this. "It is Ion Repelling"

Magnetic Arc Constriction - strong currents cause the arc to constrict, a "pinching" effect which gives rise to instabilities

To illustrate, consider a cylindrical arc column, with:

- Radius r_1
- Uniform current density

Figure 16:

Ampere's law (2.96) for steady currents is:

$$\nabla \times \vec{B} = \mu \vec{j} \quad (7.75)$$

Taking the surface integral on a closed loop around the column,

$$\int_S (\nabla \times \vec{B}) \cdot d\vec{A} = \int_S (\mu \vec{j}) \cdot d\vec{A}$$

which by Stokes's theorem (2.73) is

$$\oint_c \vec{B} \cdot d\vec{l} = \mu \int_S \vec{j} \cdot d\vec{A}$$

Forcing the closed loop to be a circle of radius r , this becomes

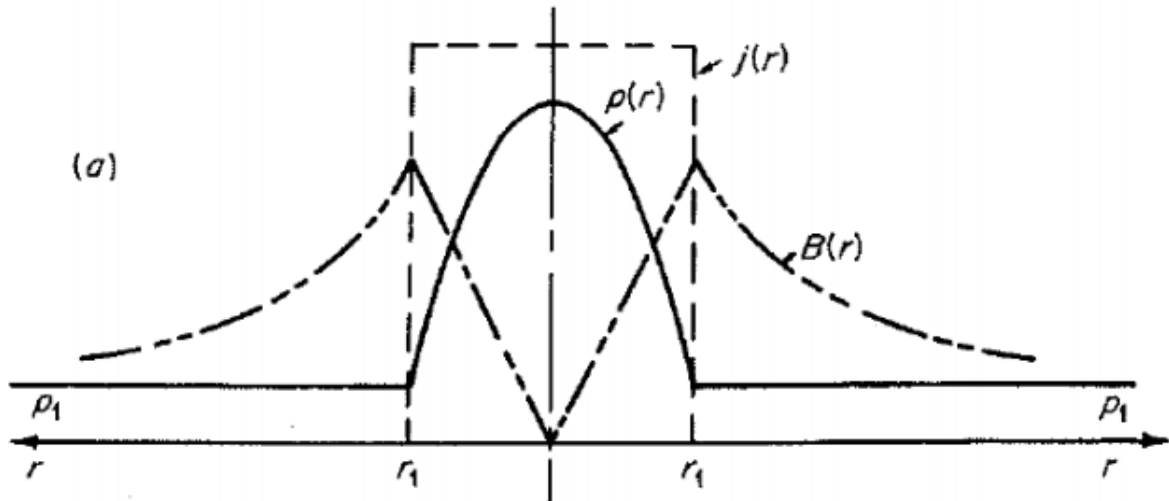
$$2\pi r B_\theta = \mu \pi r^2 j \Big|_0^{r_1}$$

So the azimuthal magnetic field strength is:

$$B_\theta = \begin{cases} \frac{\mu j r}{2} & 0 < r \leq r_1 \\ \frac{\mu j r_1^2}{2r} & r \geq r_1 \end{cases} \quad (7.76)$$

The Magnetic field profile inside and outside the arc. We have found the magnetic field but we still don't know why it pinches. The pinching is caused by a force. We are going to have a Lorentz force

This is shown in figure below (Jahn 6-16a).



Now recall the Lorentz force (2.66) with no Efield, on a single charge is:

Looking at the sketch above, if \mathbf{J} is in this direction, what direction is the magnetic field. In the direction we draw the loop. Therefore the force \mathbf{F} is going to be radially inwards.

$$\vec{F}_q = q \vec{v} \times \vec{B}$$

So the Lorentz force on a volume element dV with a number density n of charges is:

$$n \vec{F}_q dV = n q \vec{v} \times \vec{B} dV$$

or by definition of current density (2.51),

$$\vec{j} = n q \vec{v}$$

we have:

$$\vec{f} = \vec{j} \times \vec{B} \quad \left[\frac{N}{m^3} \right] \quad (7.77)$$

where we use a lower-case f to denote force density (force per unit volume). So for this arc,

$$\vec{f} = -\frac{1}{2} \mu j^2 \vec{r} \quad \text{for } r \leq r_1 \quad (7.78)$$

For all the regions we care about. There is no force outside of r_1 because there is no arc there, there is no current there.

In equilibrium, this (inward) Lorentz force density is balanced by the (outward) radial pressure gradient:

$$\frac{dp}{dr} = -\frac{1}{2} \mu j^2 \vec{r} \quad (7.79)$$

Integrating from $r = 0$ to r :

$$p(r) = p_1 + \frac{1}{4} \mu j^2 (r_1^2 - r^2) \quad (7.80)$$

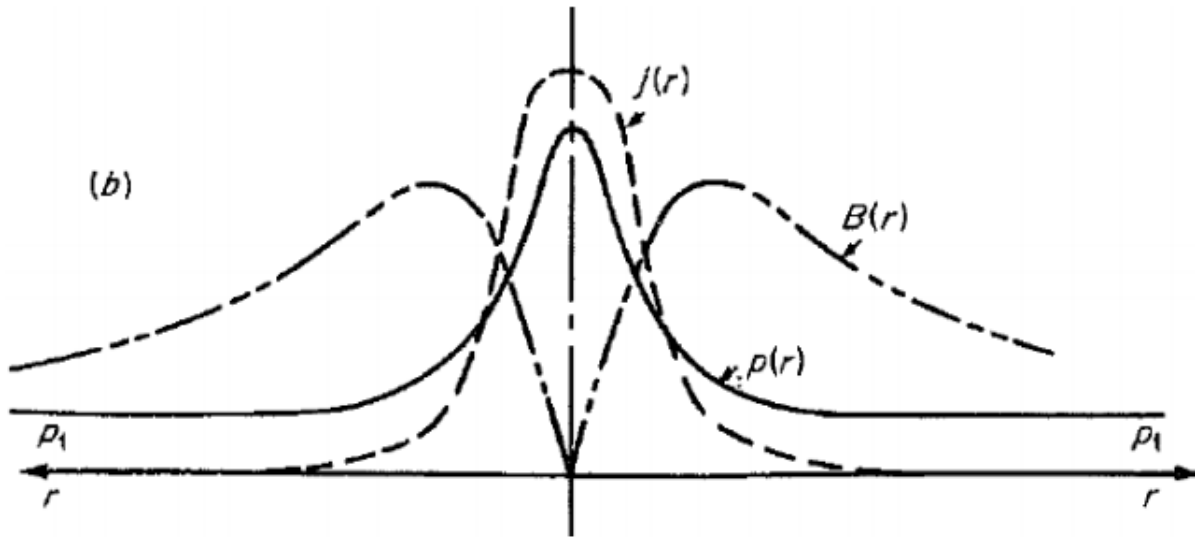
where p_1 is the ambient pressure (outside the arc). Thus the maximum pressure is at the core, on the centerline,

$$p(0) = p_1 + \frac{1}{4} \mu j^2 r_1^2 \quad (7.81)$$

The above analysis assumes UNIFORM current density.

Here's why this is unlikely:

1. The temperature distribution $T(r)$ is highest at the center, $r = 0$
2. Since $p = nkT$ for a perfect gas, $n \sim$ uniform through the arc. Both p and T increase toward centerline such that $n \sim$ constant
3. Since $j \perp B$ and $B \rightarrow 0$ at $r = 0$, the axial conductivity also peaks at $r = 0$. No Bfield on centerline to retard electron (current) motion.
4. End result: \vec{j} is generally not uniform, as shown in figure below.



Regardless of whether the current density is uniform or not uniform.

This pinching process unfortunately leads to instability. For this process there are two types of instabilities:

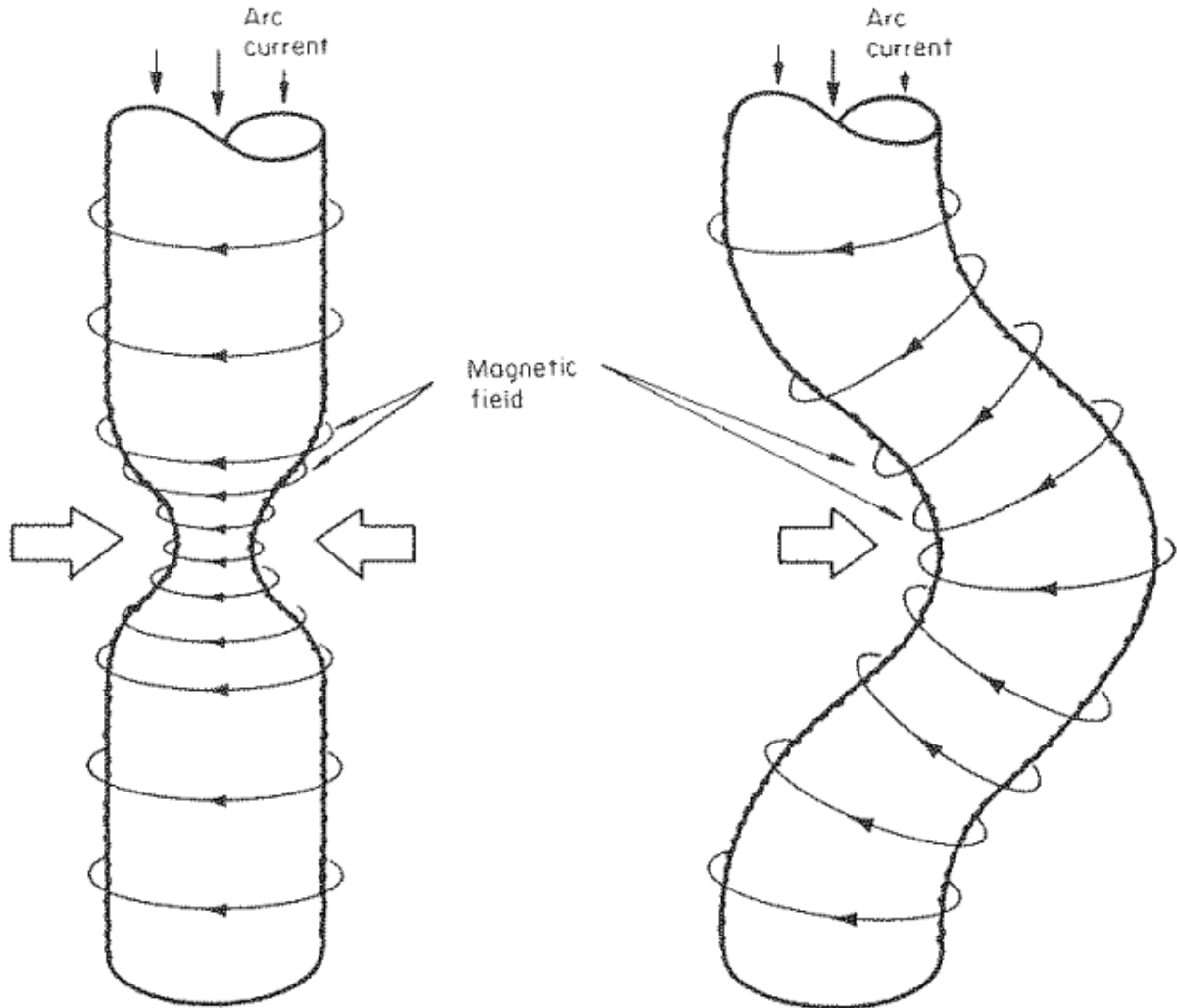


Fig. 6-17 Sausage and kink instabilities of a pinched electric arc.

1. **Sausage:** Since the arc current is:

$$J = \pi \int_0^{r_1} \vec{j}(r) r \, dr \sim r_1^2$$

The force density in a constant current arc is

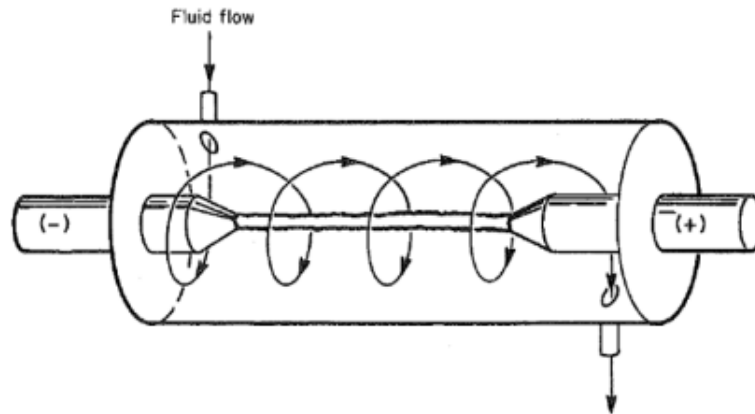
$$\vec{f} = -\frac{1}{2} \mu j^2 \vec{r} \sim -\frac{J}{r} \hat{r}$$

As a result, a small inward perturbation will grow, "necking" off the arc.

2. **Kink:** deflections of the arc tend to grow, since forces are strong at smaller radii of curvature

Three Methods for Stabilizing an Arc:**1. Axial Magnetic Field:**

Bfield confines arc to center, arc tunnels (for reentry - hypersonics studies) use this technique.

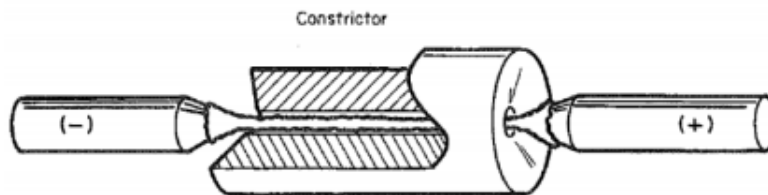
2. Gas Vortex :

In addition to stabilization, advantages include:

- Convection cools the walls
- Longer fluid path increase the residence time, get higher overall temperature
- Injected gas cools the arc, lowering its conductivity enabling higher operating voltage and higher power

3. Constriction:

The pressure inside constriction will be high which keeps the arc from bending.



2.3 Modeling Approaches

2.3.1 Core Flow Model

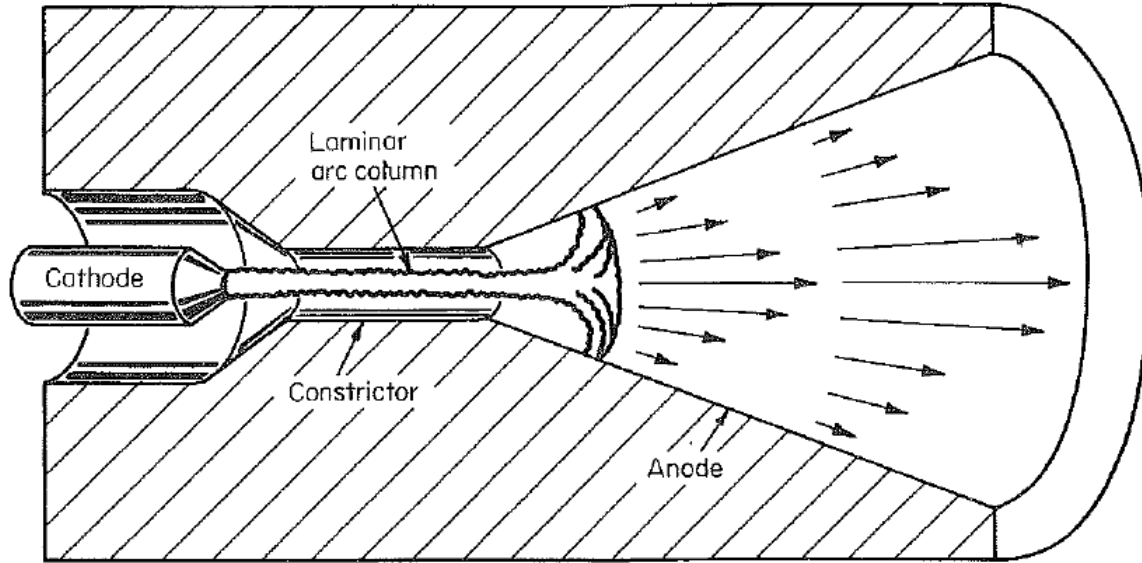


Fig. 6-22 Core-flow pattern in a constricted arcjet.

Assumptions:

- All heat input is in the arc column:

$$P_{\text{in}} = \vec{j} \cdot \vec{E} = \sigma E^2 \quad (7.82)$$

Where

σ = Electrical Conductivity

- Small diameter arc column with negligible gas flow
- Cathode heated by cathode fall (JV_c), preheating gas
- Constrictor heated by radiation from arc (optically thin gas)
- Anode heated by anode fall (JV_a) upstream, convection downstream
- Transparent column, LTE, no axial gradients

Thus the:

Energy Balance for a Core Flow Model Arc:

$$\sigma E^2 = P_{\text{radiated}} - \frac{1}{r} \frac{d}{dr} \left(r k \frac{dT}{dr} \right) \quad (7.83)$$

Where

P_r = Radiative Power Loss per Unit Volume

k = Thermal Conductivity

These are tabulated for a variety of gases, at a given T, P.

The boundary conditions on the centerline are:

$$\text{At } r = 0 \quad T(0) = T_o$$

$$\left. \frac{dT}{dr} \right|_{r=0} = 0$$

Can then solve for core temperature $T_o(E)$.

For example, Jahn calculates for hydrogen at 1 atm with $J = 150\text{A}$:

E [V/cm]	T_o [K]
25	20,000
100	40,000
250	60,000

for various voltage gradients (E) along the column. These calculations also predict an arc diameter of 1-2mm.

2.3.2 Heat Transfer:

The same model can be used to calculate the heat transfer processes within the thruster block. Expect the temperature profile to have a minima away from the walls:

Figure 17:

Why: The wall flow cools the walls, which soak up radiation from the arc.

Figure 6-23 shows thermal calculations (using core flow model) for a 30-kWe H₂ arcjet.

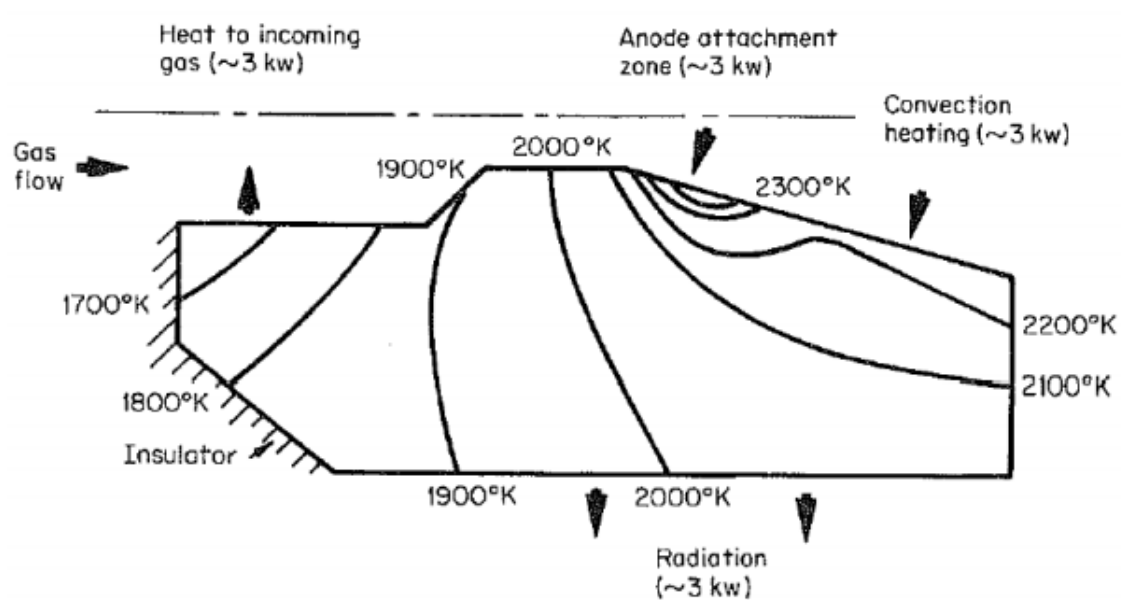


Fig. 6-23 Temperature profiles in 30-kw arcjet thruster block. (AVCO Corporation, Space Systems Division, Wilmington, Mass.)

Heat loss routes:

- 3kW to anode (by attachment and radiation)
- 3kW to nozzle (by convection)
- 3kW to the gas (by convection and conduction)
- 3kW radiated to free space (gray body, $\varepsilon \sigma T_{\text{external}}^4$)

Figure 6-24 shows that there's significant regenerative cooling/heating, even with a solid anode. In other words, there is significant heat transfer from the hot walls to the gas (like a resistojet).

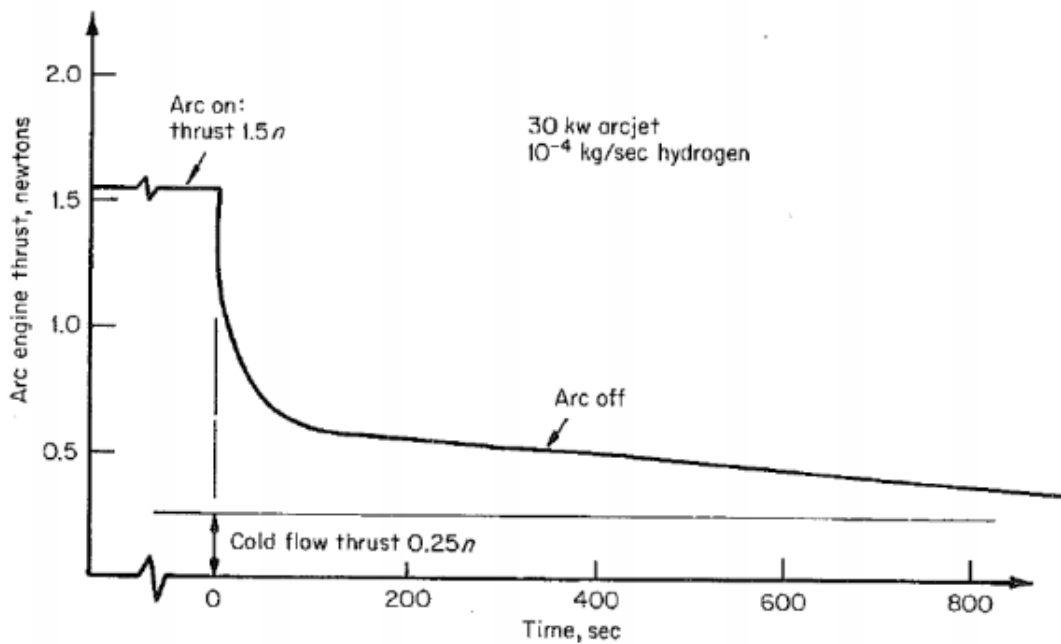


Fig. 6-24 Arcjet thrust decay after arc extinction. (From R. R. John et al., *Arc Jet Engine Performance: Experiment and Theory*, AIAA J., ser. 11, vol. 1, p. 2517, 1963.)

The slow thrust decrease is due to heat transferred from the walls to the cool gas, even after the arc is shut off.

The core flow model neglects axial enthalpy flux to high-temperature gas in the arc column. (7.83) was for radial energy flux only. Clearly there is significant axial flux of high enthalpy gas. The Stine-Watson model includes this:

Stine-Watson Model:

$$\sigma E^2 = \rho u \frac{dh}{dz} - \frac{1}{r} \frac{\partial}{\partial r} \left(r k \frac{dT}{dr} \right) \quad (7.84)$$

Note this neglects radiative losses! Instead, we can use Stine-Watson model to solve for $h(r,z)$. More sophisticated analyses take into account...

We need to solve for: Fluid dynamics in gas, Interface (sheath) models, Heat transfer to/from solid components

Meaning we need coupled equations for: Continuity, Momentum, Energy, Maxwell's Equations, Heat conduction in the solid, Constitutive relations ($\sigma(T)$, $k(T)$, $\mu(T)$)

General Equation for Arc Heating:

$$\sigma E^2 = P_r - \frac{1}{r} \frac{\partial}{\partial r} \left(r k \frac{dT}{dr} \right) - \frac{\partial}{\partial z} \left(k \frac{dT}{dz} \right) + \rho u \frac{dh}{dz} + \rho v \frac{dh}{dr} - u \frac{dp}{dz} \quad (7.85)$$

Where

P_r = Radiated power

$\frac{\partial}{\partial r} \left(r k \frac{dT}{dr} \right)$ = Radial conduction

$\frac{\partial}{\partial z} \left(k \frac{dT}{dz} \right)$ = Axial conduction

$\rho v \frac{dh}{dr}$ = Radial convection

$\rho u \frac{dh}{dz}$ = Axial convection

$u \frac{dp}{dz}$ = Pressure work

To this energy equation must be added a momentum component.

$$\rho u \frac{du}{dz} + \rho v \frac{du}{dr} = -\frac{\partial p}{\partial z} + \frac{1}{r} \frac{\partial}{\partial r} \left(r \mu \frac{du}{dr} \right)$$

Where the viscous force $\mu \frac{du}{dr}$ will, in general, be important in the constrictor because of the small duct diameter. As such, the mass flux equation

$$2\pi \int_0^{r_c} \rho u r dr = \text{constant}$$

is an appropriate equation of state for the boundary conditions on the arc axis and at the channel walls.

By adding momentum and continuity to this and get something like the models shown in the handouts. Real multiphysics model: rate chemistry, radiative losses, fluid dynamics

Megli, Krier, Burton - Thermophysics and Heat Transfer, Vol.10 No.4, 1996. Axisymmetric, steady, laminar continuum flow, two-temperature, chemical non-equilibrium model for N_2/H_2 arcjet with gas swirl injection (includes azimuthal momentum eqn).

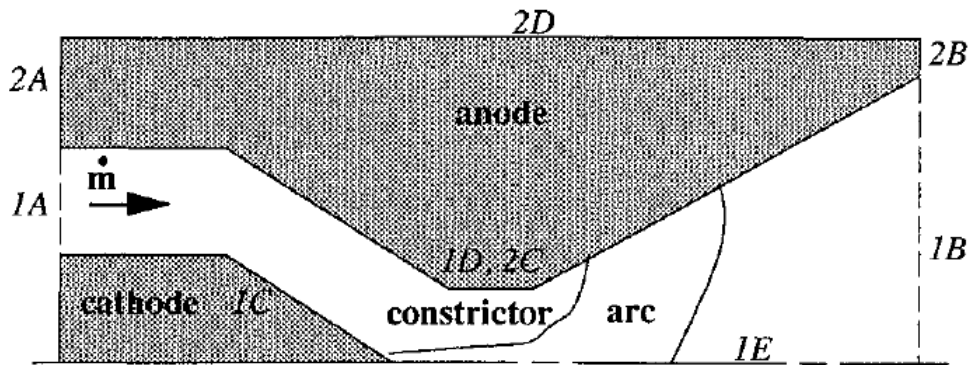


Fig. 1 Schematic of arcjet thruster indicating fluid and anode domain boundaries.

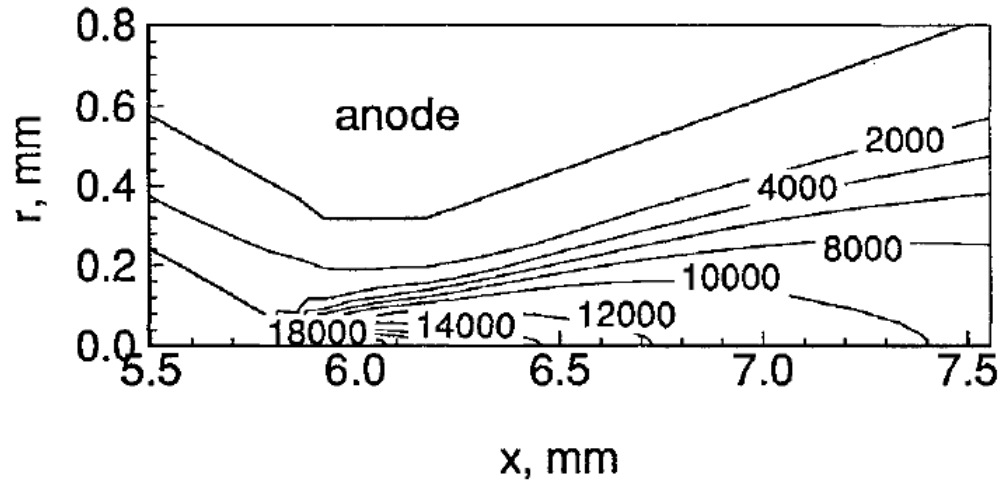


Fig. 4 T_g contours in the constrictor region. The maximum is $T_g \approx 20,000$ K at the constrictor centerline. The exit plane is located at $x = 18.4$ mm.

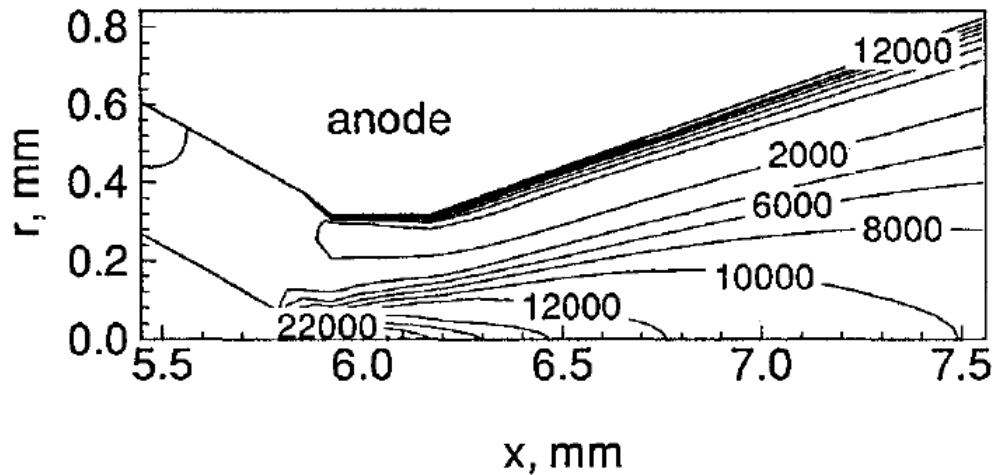


Fig. 5 T_e contours in the constrictor region. The maximum is $T_e \approx 25,000$ K at the constrictor centerline. The exit plane is located at $x = 18.4$ mm.

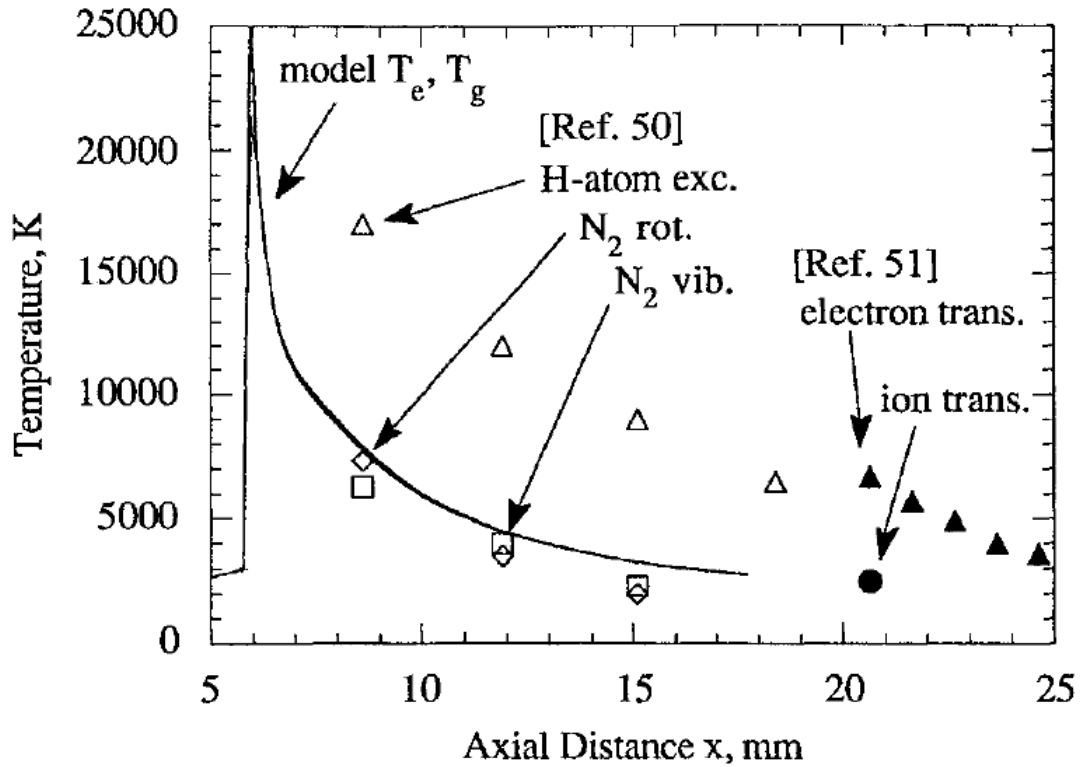


Fig. 7 Comparison of T_e and T_g temperature predictions with experimental measurements.^{50,51}

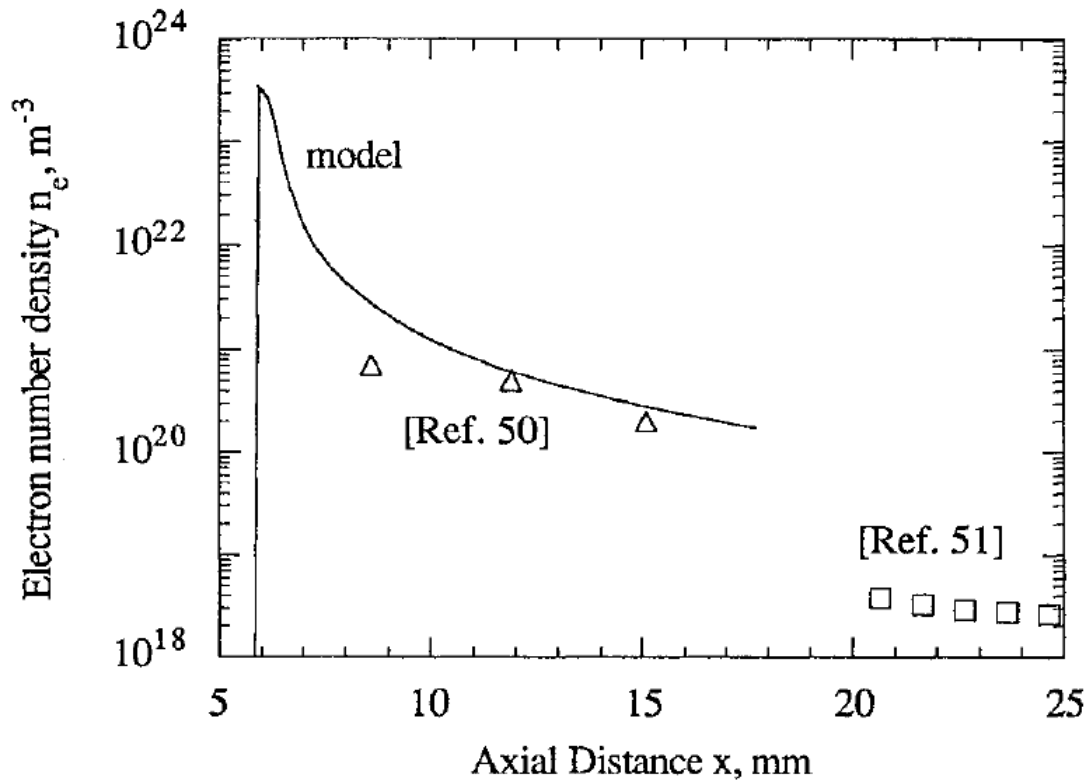


Fig. 8 Comparison of n_e predictions with experimental measurements.^{50,51}